Optical Properties of Materials for Optical Amplifiers at 1.3 µm

Hessen, B.; Sunshine, S.A.; Schneemeyer, L.F.; Neeves, A.E.; Reed, W.A.

Published in:
EPRINTS-BOOK-TITLE

Publication date:
1992

Citation for published version (APA):
Hessen, B., Sunshine, S. A., Schneemeyer, L. F., Neeves, A. E., & Reed, W. A. (1992). Optical Properties of Materials for Optical Amplifiers at 1.3 µm. In EPRINTS-BOOK-TITLE University of Groningen, Stratingh Institute for Chemistry.

OPTICAL PROPERTIES OF MATERIALS FOR OPTICAL AMPLIFIERS AT 1.3 μM

B. HESSEN, S.A. SUNSHINE, L.F. SCHNEEMEYER, A. E. NEEVES
and W.A. REED
AT&T Bell Laboratories, 600 Mountain Avenue, Murray Hill NJ 07974

ABSTRACT

We describe the preparation and near Infra-Red fluorescence characteristics of a series of transition metal (V^{2+},Ni^{2+},Cr^{4+}) doped crystalline inorganic materials. Within isostructural series, the effect of changes in the host lattice on the transition metal fluorescence has been investigated. This allows selection and fluorescence tuning of transition metal ion/crystalline host combinations of possible use for optical amplification in the 1.31 μm telecommunication window.

INTRODUCTION

The development of all-optical amplifiers based on Er^{3+}/silica [1] for signal amplification in overseas long-distance fiber connections in the 1.55 μm silica low-loss window has had a large impact on the concept of optical telecommunication networks. As yet, no comparable system has been developed for the mainly land-based networks operating in the 1.31 μm silica low-dispersion window. Systems based on Nd^{3+}/fluoride(fluorophosphate) glass, and more recently Pr^{3+}/ZBLAN, have been intensively investigated, but suffer from a number of drawbacks. The Nd^{3+} systems tend to show gain curves shifted to the long-wavelength side and away from the desired 1.31 μm by Excited State Absorption (ESA) processes [2]. The Pr^{3+} system appears to be promising, but as yet requires a high pump power due to poor quantum efficiencies and short excited state lifetimes [3]. While work progresses on these systems, it is worthwhile looking for alternative active ion/host combinations. This paper concentrates on the possible use of transition metals as active ions in systems relevant for 1.3 μm amplification.

TRANSITION METALS AS ACTIVE IONS

The transition metals differ significantly in their properties as active ions from the rare-earth ions due to their substantially stronger coupling to the host lattice. The *d*-electrons, in contrast with 4*f*-electrons, are involved in the binding of the ion to the lattice sites, and the level spacings are profoundly influenced by the crystal field imposed by the lattice. Broad lines are observed in the absorption and fluorescence spectra due to vibronic coupling, and the fluorescence wavelengths are strongly host-dependent. This strong coupling necessitates the use of crystalline rather than glassy hosts, to prevent excessive homogeneous and inhomogeneous broadening.

Single crystalline host materials offer some advantages, such as good control of site size and symmetry, and the possibility of fairly high dopant levels (usually 0.5-2 atomic% per available site). Three generic transition-metal ion/host site combinations we have considered are octahedrally coordinated V^{2+} in fluorides, octahedrally coordinated Ni^{2+} in oxides and tetrahedrally coordinated Cr^{4+} in oxides.

The optimal theoretical small-signal amplification performance of a specific active ion/host combination can be estimated from the product of the stimulated emission cross-section, σ_e, and excited state lifetime, τ, to which the gain (as expressed in dB/mW pump power) is roughly proportional. Table I lists these parameters for some already well-investigated systems. While none can match Er^{3+}/silica, it suggests that the transition metal based systems are potential candidates, since the best system for 1.3 μm operation so far, Pr^{3+}/ZBLAN, has a decidedly poor $\sigma\tau$ product.

Our studies mainly involved optically isotropic host materials (to minimize polarization problems) and investigation of the host dependence of the transition metal ion NIR fluorescence.

Table I. σ_e and τ parameters for some active-ion/host combinations

System	σ_e 10^{-20} cm^2	τ μsec	$\sigma\tau$ 10^{-19} cm^2 μsec
Er^{3+}/silica	0.5	10,000	500
Nd^{3+}/phosphate	1.13	394	45
Pr^{3+}/ZBLAN	0.35	110	3.9
Ni^{2+}/MgO	0.16	3600	58
Cr^{4+}/Mg_2SiO_4	14	3	4.2
$V^{2+}/KMgF_3$	0.4	950	38

OCTAHEDRAL VANADIUM IN FLUORIDE PEROVSKITES

Metal halide perovskites (and particularly fluorides) are known as good hosts for V^{2+} [4]. Lasing in the near IR has been reported below 200 K for $CsCaF_3:V^{2+}$ [5]. The simplicity of the structure of ABF_3 perovskites (A = monovalent, B = divalent cation), based on BF_6-octahedra sharing corners in all directions should allow for a good fluorescence-structure relation. A graph of $\lambda_{e,max}$ vs cubic cell parameter, a, is given in Figure 1, and shows a reasonably linear correlation. The graph is based on crystals of $ACaF_3:V^{2+}$ (A = K, Rb, Cs) grown by the Bridgeman technique using graphite crucibles with vanadium liners, and data from [4]. For operation in the 1.3 μm region, the smaller perovskites based on CaF_2 are preferred. Unfortunately the host material is quite hygroscopic, and growth of single crystals of good optical quality is difficult. Furthermore, the dopant is easily oxidized, and dopant level and homogeneity are difficult to control.

OCTAHEDRAL NICKEL IN OXIDE SPINELS

The spinel structure is a cubic structure with two equivalent octahedral sites and one tetrahedral site. Many spinels have the composition AB_2O_4, where the A and B cations can be distributed over the two different sites according to their preference for octahedral or tetrahedral coordination. We have prepared a series of Ni^{2+} doped spinels, as polycrystalline ceramics, and a number as single crystals, and their compositions, lattice parameters and fluorescence characteristics are listed in Table II. The observed NIR fluorescence peak varies from 1.20 μm to 1.46 μm, and the full width at half maximum is on average 0.2 μm. The fluorescence lifetime at 295 K of Ni^{2+} in spinels is typically about 0.7-0.9 ms.

A plot of the cell parameter versus the peak in the fluorescence spectrum (Figure 2) shows much less direct correlation than for the perovskites shown previously. However, some separate trends may be noticed. Replacement of the cation that preferentially occupies the octahedral site results in a fairly large incremental change in $\lambda_{e,max}$, as illustrated in the graph

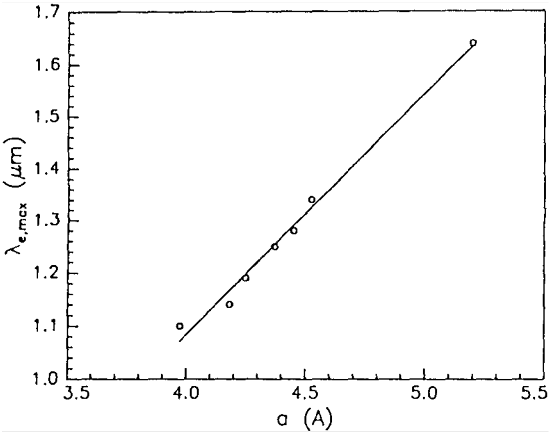

Figure 1. Fluorescence peak, $\lambda_{e,max}$, vs. cell parameter, a, for V^{2+} in halide perovskites, ABX_3.

by the Zn-containing spinels where $\lambda_{e,max}$ increases on going from Al to Ga, Ti and Sn as the ion with octahedral preference. Replacement of the cation that preferentially occupies the tetrahedral site results in a much more subtile change in $\lambda_{e,max}$, as illustrated by the Ga-spinels, where $\lambda_{e,max}$ only increases from 1.25 to 1.28 µm on changing the other ion from Li over Mg to Zn. Thus the fluorescence of octahedral Ni^{2+} in oxide spinels can be finely tuned by modification of the host lattice.

The Ni^{2+}-doped spinels have a useful pump band located around 0.9-1.0 µm and comprise a number of materials of potential interest. However, the materials are not congruently melting and have to be grown as single crystals by flux-growth techniques. The crystal growth of Ni^{2+}-doped $LiGa_5O_8$ from $PbO-B_2O_3$ based fluxes has been described, and its optical properties studied [6]. However, we noticed while growing crystals of a number of the doped materials listed above, that the luminescent properties of the crystals tended to vary slightly, and differ somewhat from the polycrystalline ceramic. Figure 3 shows the NIR luminescence spectra of three samples of $LiGa_5O_8:Ni^{2+}$. The polycrystalline ceramic has the smallest $\lambda_{e,max}$, the sample with the highest $\lambda_{e,max}$ is from the batch mentioned previously in the

Table II. Ni^{2+} in oxide spinel host materials.

Compound	Dopant	Cell (Å)	$\lambda_{e,max}$ (μm)	range (fwhm, μm)	lifetime (ms)
$ZnAl_2O_4$	Ni	8.085	1.20	1.09-1.30	
$Li_2ZnGe_3O_8$	Ni	8.191	1.27	1.17-1.41	
$LiGa_5O_8$	Ni	8.204	1.25	1.16-1.36	0.8
$MgGa_2O_4$	Ni	8.280	1.26	1.17-1.40	
$LiGaTiO_4$	Ni	8.290	1.37	1.23-1.56	
$ZnGa_2O_4$	Ni	8.335	1.28	1.17-1.44	0.9
Mg_2TiO_4	Ni	8.441	1.44	1.29-1.61	
Zn_2TiO_4	Ni	8.460	1.44	1.31-1.58	
Zn_2SnO_4	Ni	8.657	1.46	1.35-1.60	

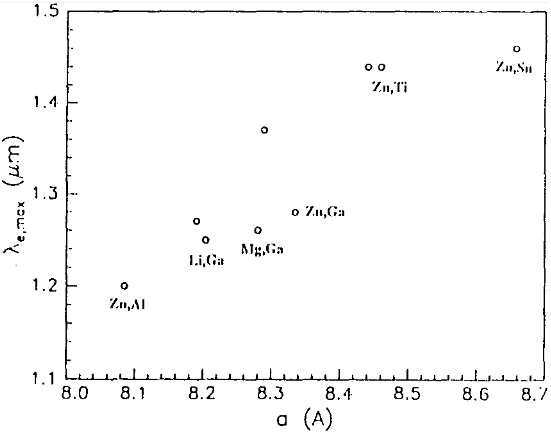

Figure 2. Fluorescence peak, $\lambda_{e,max}$, vs. cell parameter, *a*, for Ni^{2+} in oxide spinels.

literature. EDX suggests that a certain amount of Pb is incorporated into the crystals, which may result in a slight expansion of the lattice. The exact lattice parameters of the individual batches of crystals has not been determined as yet. It seems, however, that care has to be taken in the flux crystallization process to obtain material with the same optical characteristics reproduceably.

TETRAHEDRAL CHROMIUM IN VARIOUS OXIDE HOSTS

Recently, interesting NIR lasing behavior has been observed in materials containing Cr^{4+} in tetrahedral lattice sites, such as Mg_2SiO_4:Cr and $Y_3Al_5O_{12}$:Cr/Ca [7,8]. A problem in preparing these materials is that chromium prefers to occupy an octahedral site as Cr^{3+} rather than a tetrahedral site when given the choice. This implies that either host materials without octahedral sites have to be used, or that Cr has to be induced to take a tetrahedral site by charge-compensation through codoping and materials preparation in oxidizing atmosphere. We have prepared a number of Cr^{4+} doped oxide materials whose structural and fluorescence characteristics are listed in Table III. As in other previously reported Cr^{4+}-doped oxides, the excited lifetimes are short, typically shorter than 5 µs at 295 K.

Single crystal fibers of Cr^{4+}-doped $Y_3Al_5O_{12}$ (YAG) and $Ca_2Al_2SiO_7$ were grown by the Laser Heated Pedestal Growth (LHPG) method [9] (as small as 40 µm diameter). Large single crystal boules of Y_2SiO_5:Cr (YOS) were grown by the Czochralski technique [10].

Table III. Cr^{4+} in various host materials.

Compound	dopant	Cell	λ_e, max (µm)	range (fwhm, µm)
Mg_2GeO_4	Cr	ortho	1.19	1.13-1.31
$LiGaSiO_4$	Cr	trigon	1.23	1.14-1.34
Y_2SiO_5	Cr	monocl	1.23	1.14-1.36
$Ca_2Al_2SiO_7$	Cr	tetrag	1.24	1.15-1.43
$Y_3Al_5O_{12}$	Cr/Ca	cubic	1.34	1.20-1.46
Zn_2SiO_4	Cr	trigon	1.42	1.25-1.60

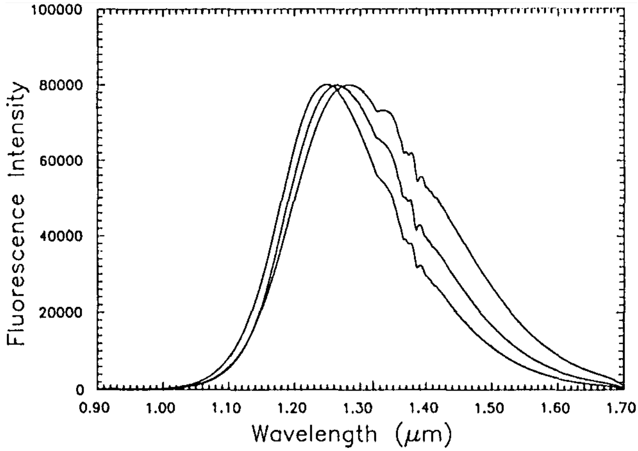

Figure 3. Fluorescence spectra for $LiGa_5O_8:Ni^{+2}$ from a ceramic sample and two different flux-grown single crystal batches.

The latter appears to be an interesting material for potential operation in the 1.3 μm range, as the ambient temperature lasing wavelengths in Cr^{4+}-doped laser materials appears to be shifted to longer wavelengths relative to the peak in the fluorescence spectrum. A disadvantage is that the material is quite anisotropic, showing pronounced dichroism.

CONCLUSIONS

A significant number of transition metal ion/crystalline host combinations exhibit NIR fluorescence around 1.3μm, and are of interest as potential alternatives for optical amplification in this wavelength region. The sensitivity of the luminiscence wavelength to changes in the host lattice allows optimization of the fluorescence characteristics for this purpose. For an evaluation of their performance in optical amplification, the preparation of small-core waveguides in the doped single crystal materials is necessary. Several useful techniques to this end are available, such as the use of light-ion implantation for local refractive index lowering. Recent interesting results with this technique on metal oxide single crystal materials include channel waveguides in $YAG:Nd^{3+}$ [11] and cladding of $LiNbO_3$ single crystal fibers [12].

ACKNOWLEDGEMENT

We wish to thank P.C. Becker and A.G. Prosser for stimulating discussions, and C.D. Brandle for providing us with boules of YOS:Cr.

REFERENCES

[1] R.J. Mears, L. Reekie, I.M. Jauncey, D.N. Payne, Electron. Lett. **23**, 1026 (1987); E. Desurvire, J.R. Simpson, P/C. Becker, Opt. Lett. 12, 888 (1987).

[2] W.J. Miniscalco, J.L. Andrews. B.A. Thompson, R.S. Quimby, L.J.B. Vacha, M.G. Drexhage, Electron. Lett. **24**, 28 (1988); M. Brierley, S. Carter, P. France, J.E. Pedersen, ibid., **26**, 329 (1990).

[3] Y. Ohishi, T. Kanamori, T. Kitagawa, S. Takahashi, E. Snitzer, G.H. Siegel Jr., OFC ’91 (San Diego), Postdeadline paper PD-2; Y. Ohishi, T. Kanamori, T. Nishi, S. Takahashi, IEEE Photon. Technol. Lett. **3**, 715 (1991).

[4] W. Knierim, A. Honold, U. Brauch, U. Dürr, J. Opt. Soc. Am. B **3**, 119 (1986).

[5] U. Brauch, U. Dürr, Opt. Commun. **55**, 35 (1985).

[6] J.F. Donegan, F.J. Bergin, T.J. Glynn, G.F. Imbusch, J.P. Remeika, J. Lumin. **35**, 57 (1986).

[7] V. Petricevic, S.K. Gayen, R.R. Alfano, K. Yamagichi, H. Anzai, Y. Yamaguchi, Appl. Phys. Lett. **52**, 1040 (1988); V. Peticevic, S.K. Gayen, R.R. Alfano, Opt. Lett. **14**, 14 (1989).

[8] N.B. Angert, N.I. Borodin, V.M. Garmash, V.A. Zhitnyuk, A.G. Okhrimchuk, O.G. Siyuchenko, A.V. Shestakov, Sov. J. Quantum Electron. **18**, 73 (1988).

[9] C.A. Burrus, J. Stone, Appl. Phys. Lett. **26**, 318 (1975); R.S. Feigelson, J. Crystal Growth **79**, 669 (1986).

[10] C.D. Brandle, A.J. Valentino, G.W. Berkstresser, J. Crystal Growth **79**, 308 (1986).

[11] S.J. Field, D.C. Hanna, D.P. Shepherd, A.C. Tropper, P.J. Chandler, P.D. Townsend, L. Zhang, IEEE J. Quant. Electron. **27**, 428 (1991).

[12] D.P.S. Saini, Y. Shimoji, R.S.E.Chang, N. Dieu, Optics Lett. 16, 1074 (1991).